TG 335-4

APRIL 1960

VIBRATIONS OF THICK-WALLED

HOLLOW CYLINDERS

EXACT NUMERICAL SOLUTIONS

J. F. BIRD, R. W. HART, and F. T. McCLURE

THE JOHNS HOPKINS UNIVERSITY

APPLIED PHYSICS LABORATORY

TG 335-4
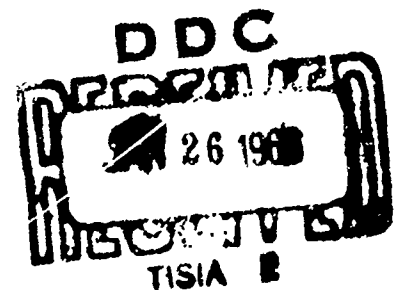
APRIL 1960

VIBRATIONS OF THICK-WALLED HOLLOW CYLINDERS EXACT NUMERICAL SOLUTIONS

J. F. BIRD, R. W. HART, and F. T. McCLURE

TABLE OF CONTENTS

ABSTRACT

The plane strain vibration frequencies of an infinitely long hollow cylinder are calculated exactly with the aid of a high-speed electronic computer, for a range of wall thicknesses and azimuthal node numbers, and for a variety of boundary conditions. These latter cover the cases: outer radial surface free, or supported, or clamped; inner surface free, or supported, or matched to a gas filling the inner cavity. In the last case, we calculate the attenuation of sound in the cylinder wall, in addition to the eigenfrequencies. Our computations of mode frequencies disclose that: (i) the shear-compressional wave coupling in the solid is very weak (except for low frequency); (ii) for the gas-filled cylinder, the modes are very close either to the gas quasi-modes (gas in a rigid-walled cylinder), or to the solid quasi-modes (shell with free inner surface), depending on the geometry.

I. INTRODUCTION

A fundamental problem of the classical theory of elasticity is the determination of the normal modes of elastic vibration of a hollow cylinder. In principle, this problem is solved by writing down the solution of the elastic wave equation and then determining the mode frequencies by the requirement that an appropriate set of boundary conditions be fulfilled. In practice, the problem is unfortunately not so simple.

The major difficulty is that the determination of the characteristic frequencies generally requires an enormous amount of numerical work, particularly because the secular equation involves cylinder functions whose arguments

depend on the frequency to be computed. Since the cylinder problem possesses a multitude of independent parameters (cylinder wall thickness, elastic constants, and wave numbers) and since a considerable number of sets of boundary conditions must be investigated, it is clear that a complete solution of the problem would involve a formidable program of numerical computation.

Of course, in simple special cases, it is possible to obtain the modes for any wall thickness from the exact theory, without undue labor. Such calculations previously have been done for the purely radial dilational modes of free, infinitely long cylinders,[1] and for the purely axial shear modes of free and clamped infinite cylinders.[2]

Now it is feasible, with electronic computers, to calculate exactly the vibration modes for thick-walled cylinders in other cases as well. Already Herrmann and Mirsky[3] have presented such calculations for axially symmetric longitudinal waves in free, infinitely long cylinders. They gave numerical results for the lowest mode and a range of wall thicknesses. Greenspon[4]

---

[1] G. S. Field, Can. J. Research A 17, 141 (1939); J. A. McFadden, J. Acoust. Soc. Am. 26, 714 (1954); A. B. Bassett, Proc. London Math. Soc. 21, 53 (1889).

[2] J. H. Baltrukonis and W. G. Gottenberg, J. Acoust. Soc. Am. 31, 734 (1959).

[3] G. Herrmann and I. Mirsky, J. Appl. Mech., Trans. Am. Soc. Mech. Engrs. 78, 563 (1956), 79, 1 (1957).

[4] J. E. Greenspon, J. Acoust. Soc. Am. 31, 1682 (1959), J. Aero. Space Sci. 27, 37 (1960).

calculated the lowest few flexural modes for free, infinitely long cylinders. In addition, he has treated the flexural modes of the finite length cylinder, again with free sides, but with ends either free or freely-supported. More recently, Gazis has published extensive calculations for the infinite hollow cylinder which is stress-free at both inner and outer radial surfaces - first, for plane-strain vibrations, later for the general case involving axial motion also.[5] He considered a range of geometries and axial wavelengths and several values of the azimuthal quantum number for the lowest dozen modes or so.

The purpose of the present paper is to calculate exactly the eigenfrequencies of the infinite length thick-walled cylinder for boundary conditions not treated in the above work (refs. 3, 4, 5), i.e., for other than stress-free radial surfaces. In these computations, we shall consider plane-strain vibrations in the infinite hollow cylinder for a range of wall thicknesses. For these modes, however, we shall extend Gazis' work as follows.

First of all, the infinite hollow cylinder will be treated for a number of new combinations of boundary conditions of the usual type. Thus, we shall consider the outer surface to be either clamped, r supported, or free, while the inner surface is either supported, or free. These investigations lead to the discovery that the thickness eigenmodes[6] are generally either almost purely radial dilatational or almost purely azimuthal shear. The frequencies of these modes are

---

[5]D. C. Gazis, J. Acoust. Soc. Am. 30, 786 (1958), 31, 568, 573 (1959).

[6]These are modes with at least one displacement node or antinode occurring across the thickness of the cylinder wall.

in fact very nearly the same as for the corresponding pure modes. This indicates that the shear-compression coupling is quite weak for such modes.

Secondly, we shall consider the very interesting situation of a gas filling the inner part of the cylinder, [7,8] while the outer surface is again either clamped, or supported, or free. In this case we are dealing with the acoustic modes of a two-phase system, where no matter how tenuous the gas inside the cylinder may be, the modes of the system are often drastically different from those calculated by neglecting the presence of the gas. We find that, depending on the ratio of inner to outer radius, the eigenmodes are very closely similar either to the modes of a shell with free inner surface (solid quasi-mode) or to the modes of a gas in a rigid-walled cylinder (gas quasi-mode).

---

[7] Some special examples of this case have been given previously in a theoretical treatment of the problem of combustion instability in a rocket motor charged with an inside-burning tubular grain. See, (a) F. T. McClure, R. W. Hart, and J. F. Bird, J. Appl. Phys. (scheduled for publication in May 1960), and (b) F. T. McClure, R. W. Hart, and J. F. Bird, Proceedings of the Princeton-A.R.S. Solid Propellant Research Symposium (Jan. 28, 29, 1960).

[8] Other such two-phase systems have been treated previously by C. Sălceanu and M. Zăgănescu, Compt. rend. 247, 812 (1958) and F. I. N. Niordson, Trans. Roy. Inst. Tech. Stockholm, no. 73 (1953) for very simple cases, and by R. D. Fay, J. Acoust. Soc. Am. 24, 459 (1952) with a vitiating error. Also see M. A. Biot, J. Appl. Phys. 23, 997 (1952).

Finally, as a rather novel application of elasticity theory, we compute exactly the attenuation of sound in the solid wall for the gas-filled cylinder, by only slightly extending the eigenfrequency computation program.

II. DISPLACEMENT AND STRESS IN CYLINDER

Here, we shall merely display the form of the solution, since the methods of derivation are standard procedure and readily available elsewhere.[9] In the notation of ref. 7, we have for the displacement vector $\underset{\sim}{S}$, and stress tensor, $\underset{\approx}{P}$, the following components:

$$S_r = + i\,e^{i\omega t}\cos(m\varphi)\left\{A_1 J'_m(k_c r) + A_2 Y'_m(k_c r)\right.$$
$$\left. + \frac{m}{k_s r}[B_1 J_m(k_s r) + B_2 Y_m(k_s r)]\right\} \tag{1}$$

$$S_\varphi = - \frac{i\,m e^{i\omega t}}{k_c r}\sin(m\varphi)\left\{A_1 J_m(k_c r) + A_2 Y_m(k_c r)\right.$$
$$\left. + \frac{k_c r}{m}[B_1 J'_m(k_s r) + B_2 Y'_m(k_s r)]\right\} \tag{2}$$

$$P_{rr} = - \frac{i2\mu e^{i\omega t}}{r}\cos(m\varphi)\left\{A_1 j_r(k_c r) + A_2 y_r(k_c r)\right.$$
$$\left. + B_1 j_1(k_s r) + B_2 y_1(k_s r)\right\} \tag{3}$$

$$P_{r\varphi} = + \frac{i2\mu e^{i\omega t}}{r}\sin(m\varphi)\left\{A_1 j_1(k_c r) + A_2 y_1(k_c r)\right.$$
$$\left. + B_1 j_\varphi(k_s r) + B_2 y_\varphi(k_s r)\right\} \tag{4}$$

---

[9] P. M. Morse and H. Feshbach, Methods of Theoretical Physics (McGraw-Hill Book Company, Inc., New York, 1953), pp. 142, 1840.

where

$$j_1(x) = m \left[\frac{J_m(x)}{x} - J'_m(x) \right] , \qquad (5)$$

$$j_r(x) = J'_m(x) + x J_m(x) \left[1 + \frac{\frac{\lambda}{2\mu} (k_c r)^2 - m^2}{x^2} \right] , \qquad (6)$$

$$j_\varphi(x) = J'_m(x) + x J_m(x) \left(\frac{1}{2} - \frac{m^2}{x^2} \right) , \qquad (7)$$

and the y functions similar but with $J_m \longrightarrow Y_m$. Also, we have used,

$$k_c^2 = \frac{\omega^2}{c_d^2} , \qquad k_s^2 = \frac{\omega^2}{c_s^2} , \qquad (8a)$$

with the familiar relationships

$$c_d = \sqrt{\frac{\lambda + 2\mu}{\rho}} \qquad \text{and} \qquad c_s = \sqrt{\frac{\mu}{\rho}} , \qquad (8b)$$

where λ and μ are the Lamé elastic moduli, ρ is the density of the solid cylinder, and m is the (integer) angular wave number. The determination of the amplitudes A_1, A_2, B_1, B_2 by applying the boundary conditions accomplishes the solution to the problem.

III. THE BOUNDARY CONDITIONS

In this section we specify the various sets of boundary conditions that we shall apply to the displacement and stress functions, Eqs. (1-4) a the inner and outer boundaries of the cylinder, i.e., at r = a, r = b. (Since the cylinder length is infinite, we apply no boundary conditions on planes perpendicular to the z-axis.)

1. Conditions on Outer Cylindrical Surface

On this surface $r = b$, we shall apply any one of the three sets of conditions

$$P_{rr} = P_{r\varphi} = 0, \text{ at } r = b, \tag{9a}$$

$$S_r = P_{r\varphi} = 0, \quad \text{at } r = b, \tag{9b}$$

$$S_r = S_\varphi = 0, \quad \text{at } r = b, \tag{9c}$$

corresponding to free, supported, or clamped ouside surface, respectively.

2. Conditions on Inner Cylindrical Surface

The inner surface ($r = a$) of the hollow cylinder we shall consider to be either free

$$P_{rr} = P_{r\varphi} = 0, \text{ at } r = a , \tag{10a}$$

or supported

$$S_r = P_{r\varphi} = 0, \text{ at } r = a, \tag{10b}$$

or to match in both stress and displacement to a gas filling the inside of the cylinder. Assuming the gas exerts no tractive force on the solid surface, this last case requires

$$P_{rr} + i \omega Z_g S_r = P_{r\varphi} = 0, \text{at } r = a \tag{10c}$$

where Z_g is the acoustic impedance for the gas at the boundary wall, $Z_g \equiv [p/u]_{r=a}$, with p, u being acoustic pressure and radial particle velocity in the gas. With acoustic gas pressure of the form $p_o e^{i\omega t} \cos (m\varphi) J_m(k_g r)$, we have from $u = \dfrac{i}{\rho_g \omega} \dfrac{\partial p}{\partial r}$ that the impedance is

$$Z_g = - i\rho_g c_g J_m(k_g a)/J'_m(k_g a) \tag{11}$$

where ρ_g is gas density, and $k_g = \omega/c_g$, with c_g being sound velocity in gas. We note that Eqs. (10a), (10b) are special cases of (10c), for $Z_g \rightarrow 0$ and $Z_g \rightarrow \infty$, respectively.

When we apply these various sets of boundary conditions to the elastic wave described by the displacement and stress of Eqs. (1) -- (4) , we will find in each case that four simultaneous equations which are linear and homogeneous in the constants A_1, A_2, B_1, B_2, need to be satisfied. For a non-trivial solution, the determinant formed from the coefficients of the A's and B's must be zero. This condition determines the eigenfrequencies of the system, so that in the following we are to be concerned with finding the frequency roots of this secular determinant for each set of boundary conditions.

IV. DIMENSIONS AND PHYSICAL CONSTANTS OF THE SYSTEM

The secular equation for the oscillation frequencies ($f = \omega/2\pi$) will in general involve the dimensions $\underline{a}$, $\underline{b}$, of the cylinder, and the density and elastic constants of both the cylinder and the gas inside the cylinder. For the empty cylinder, these quantities fall into three dimensionless groups, a/b, $\omega b/c_s$, and σ (Poisson's ratio); for the gas filled cylinder, two additional parameter groups appear, namely ρ_g/ρ, and c_g/c_s. Clearly, a complete investigation over the whole parameter field would require an undesirably large effort. In this modest investigation, we have confined our attention to a study of the dependence on only a/b and $\omega b/c_s$, while selecting the constants $\sigma = 0.38$, $\rho_g/\rho = 1/160$, and $c_g/c_s = 10/3.08$ as representative values of the remaining quantities. Rather than present the results in terms of the two dimensionless parameters which we have considered, however, we elect to display the mode frequencies as a

function of inner radius for a selected value of b, and c_s, because we believe that this presentation facilitates a more concrete feeling for the nature of the results. We shall use b = 5.75 cm, c_s = 3.08 x 10^4 cm/sec. (These values correspond to λ = 4.813 x 10^8 dyne/cm^2 and μ = 1.52 x 10^9 dyne/cm^2). Finally, in our illustrative calculations of sound attenuation in the solid wall, we shall use the dilatational and shear viscosities λ^1 = 200 poise, η = 200 poise, respectively.[7]

V. EXACT NUMERICAL EIGENFREQUENCIES

1. Clamped, Supported and Free Boundaries

Here we present our results for the six sets of boundary conditions specified by Eqs. (9), (10a), (10b), viz., outer surface either clamped or supported or free, inner surface either supported or free.

The characteristic frequencies were calculated on the "Univac-Scientific" for several values of $\underline{m}$. Roots were sought for frequencies up to 25,000 cps, corresponding to $\omega b/c_s \leq$ 29.4. The method of computation was to select a value of $\underline{a}$ and then calculate the determinantal roots by an interval-halving technique. Doing this for about 10 values of $\underline{a}$ from 2.87 to 5.75 cm was sufficient to give the mode-maps for these cases, since the curves are smooth. These results are shown in Figs. 1 to 6, as graphs of frequency vs inner radius/outer radius.

Fig. 1 shows the plane-strain modes of the completely free cylinder (cf. refs. 4,5). Those modes such that the frequency $\underline{f}$ becomes infinite as $\underline{a} \rightarrow \underline{b}$ are the thickness modes defined in Sec. I. We follow Gazis[4] in calling the remaining pair of modes "ring modes". Figures 2-6 illustrate how different
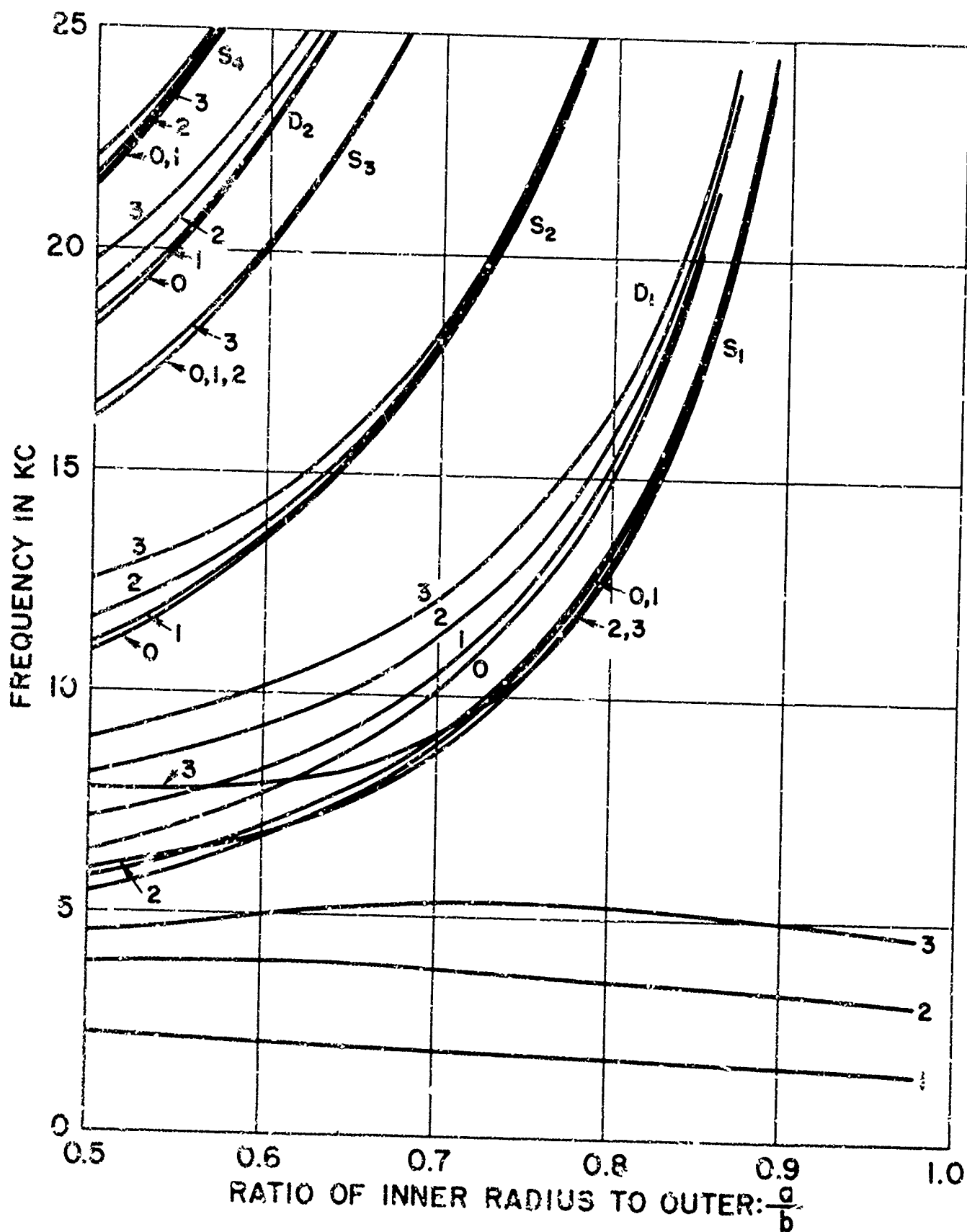
Fig. 1 FREQUENCY VERSUS GEOMETRY FOR THE m = 0, 1, 2 AND 3
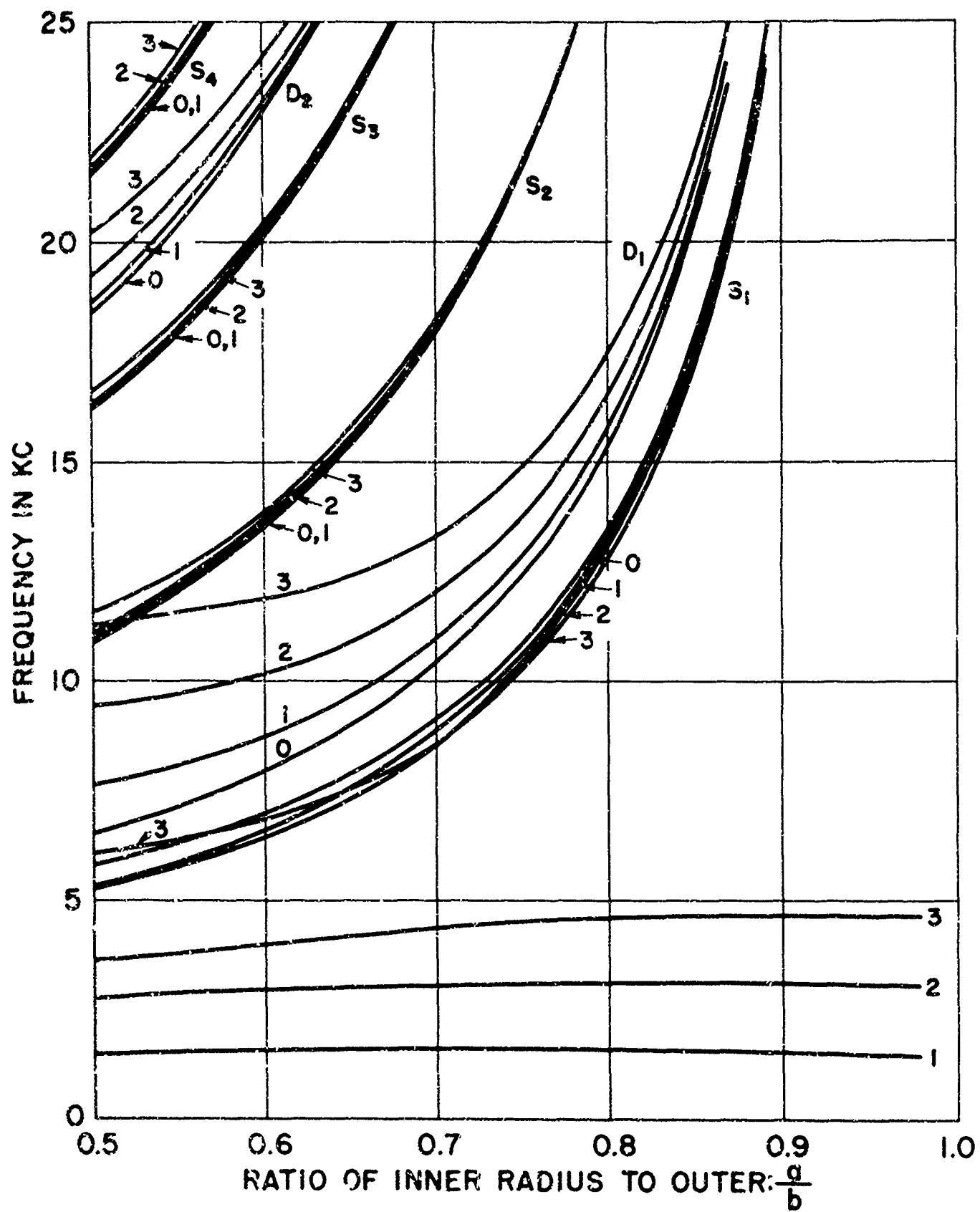MODES OF A SOLID CYLINDRICAL SHELL WITH OUTER SURFACE
FREE AND INNER SURFACE FREE

Fig. 2 FREQUENCY VERSUS GEOMETRY FOR THE m = 0, 1, 2 AND 3
MODES OF A SOLID CYLINDRICAL SHELL WITH OUTER SURFACE
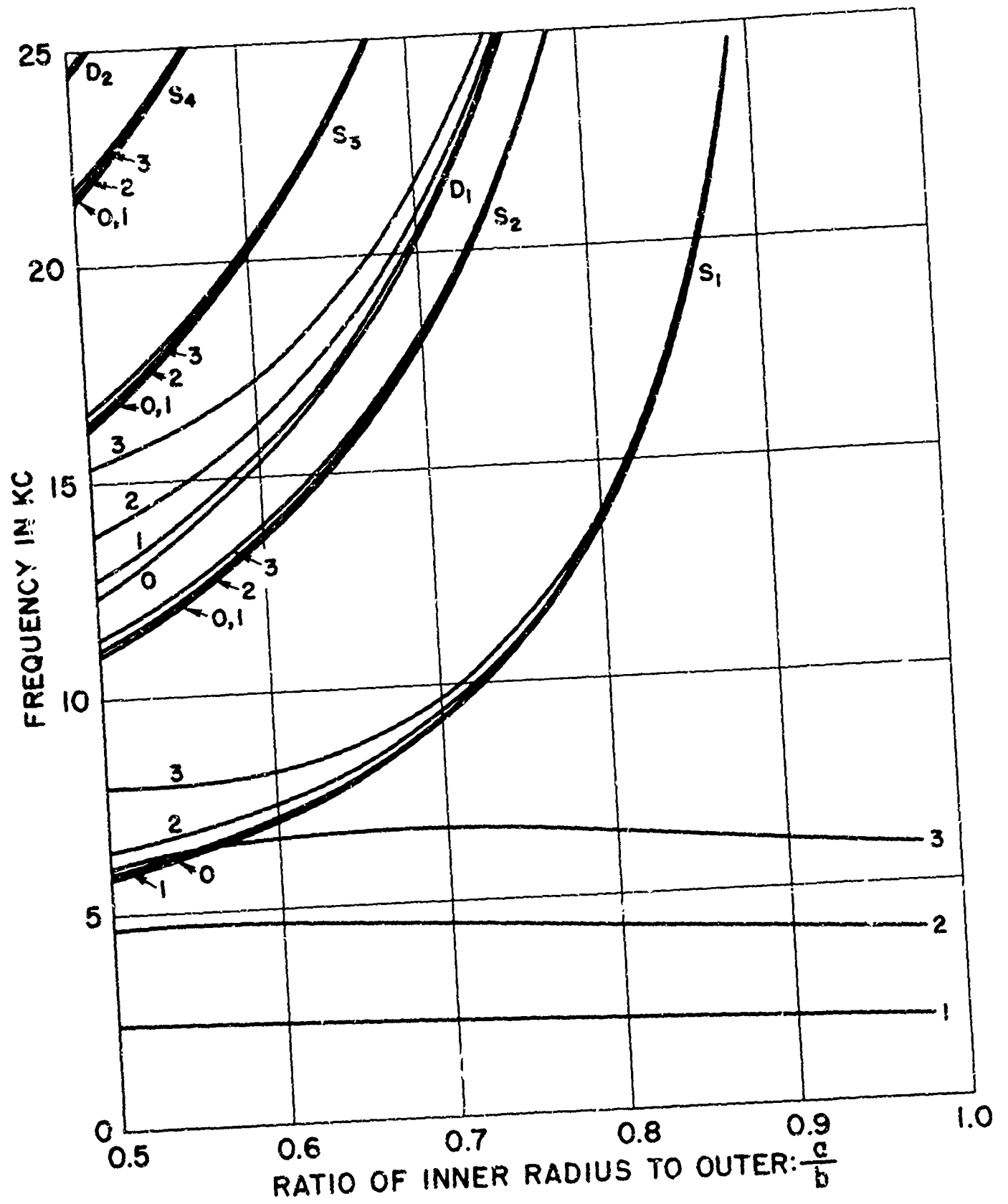FREE AND INNER SURFACE SUPPORTED

Fig. 3 FREQUENCY VERSUS GEOMETRY FOR THE m = 0, 1, 2 AND 3 MODES OF A SOLID CYLINDRICAL SHELL WITH OUTER SURFACE SUPPORTED AND INNER SURFACE SUPPORTED
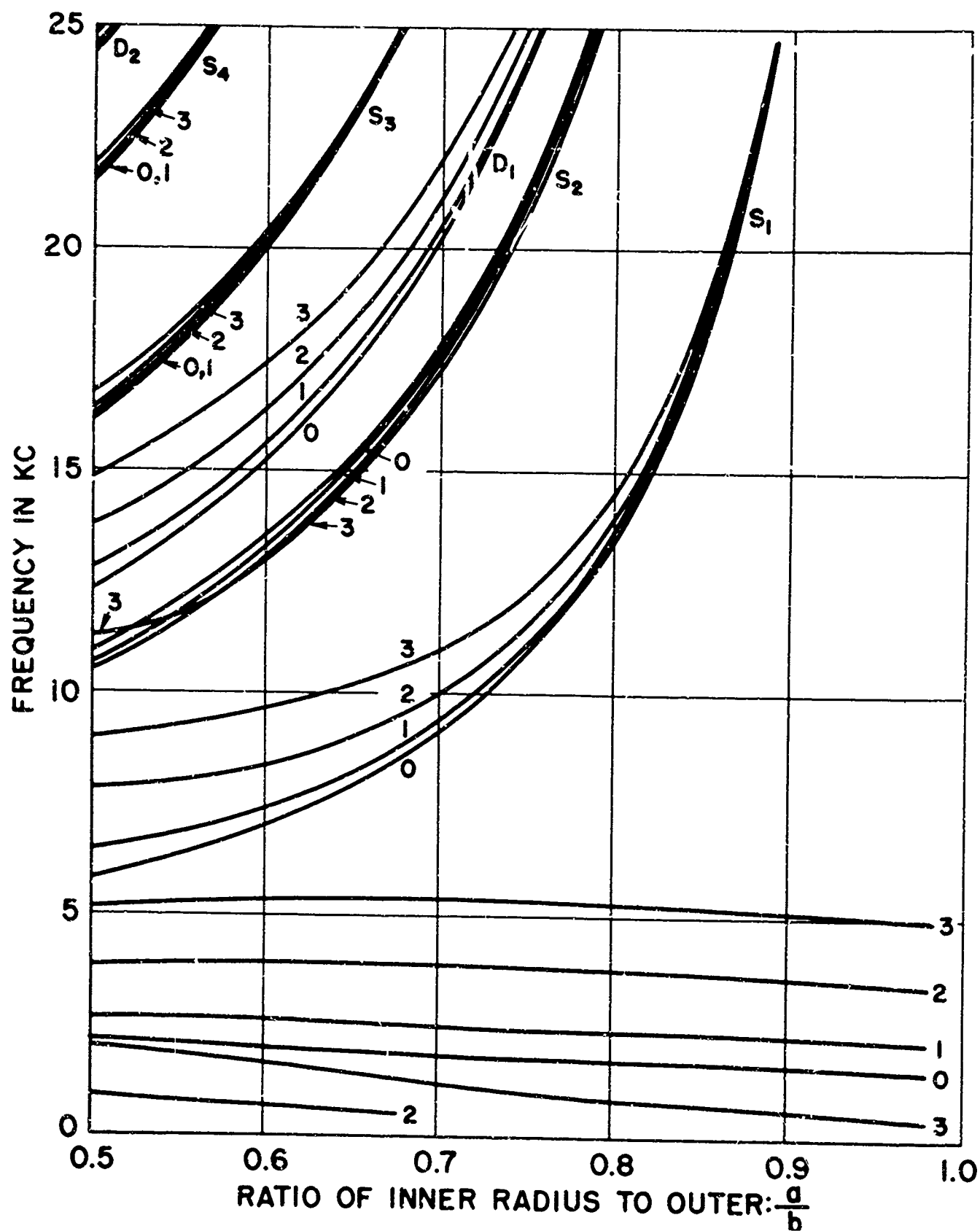
Fig. 4 FREQUENCY VERSUS GEOMETRY FOR THE m = 0, 1, 2 AND 3
MODES OF A SOLID CYLINDRICAL SHELL WITH OUTER SURFACE
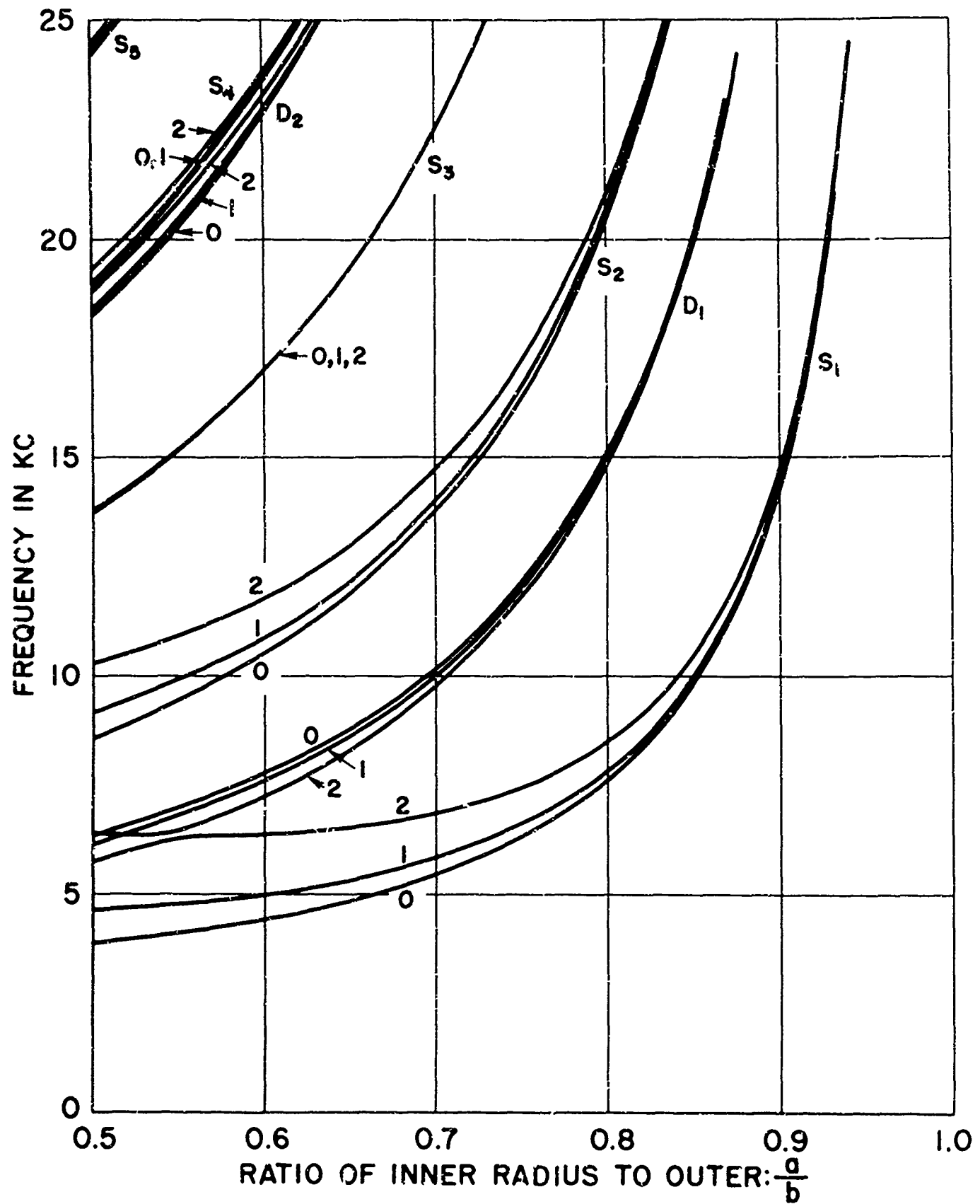SUPPORTED AND INNER SURFACE FREE

Fig. 5 FREQUENCY VERSUS GEOMETRY FOR THE m = 0, 1 AND 2
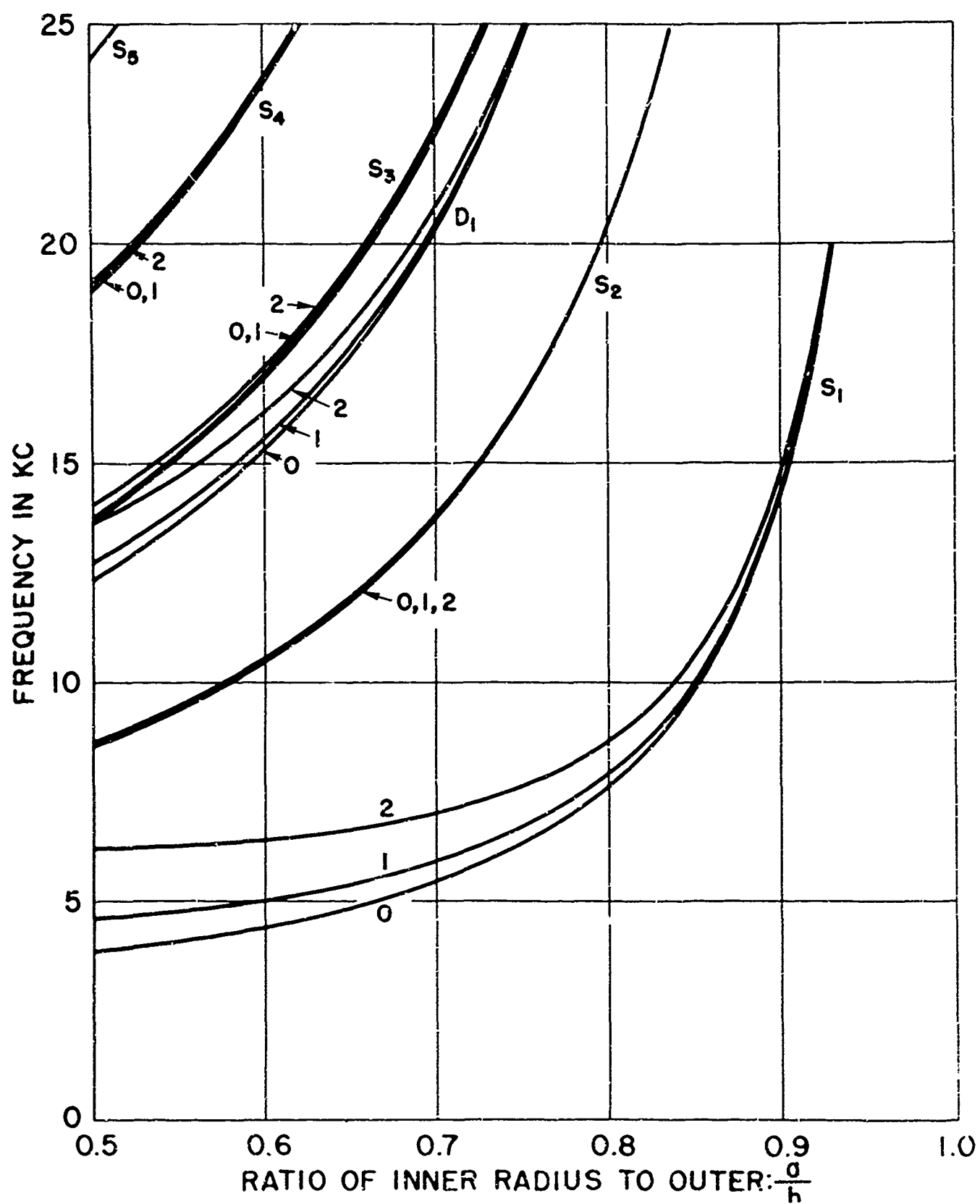MODES OF A SOLID CYLINDRICAL SHELL WITH OUTER SURFACE
CLAMPED AND INNER SURFACE FREE

Fig. 6 FREQUENCY VERSUS GEOMETRY FOR THE m = 0. 1 AND 2
MODES (A SOLID CYLINDRICAL SHELL WITH OUTER SURFACE
CLAMPED AND INNER SURFACE SUPPORTED

sets of boundary conditions affect both thickness and ring modes.

Consider first the ring modes. The lower of these in Fig. 1 is a flexural mode, which has non-zero frequency only for $m \geq 2$, while the upper is an extensional ("breathing") mode.[4] For each of Figs. 2-6, the extensional freedom is removed ($S_r = 0$ at $r = a$ and/or $r = b$) and the ring-extensional mode disappears. In Figs. 5 and 6 the ring-flexural mode is also absent, since the flexural freedom has been removed ($S_\varphi = 0$ at $r = b$). Note that for Figs. 2, 3, and 4 the ring-flexural mode has zero frequency only for $m = 0$.

The thickness modes also exhibit a regular behavior as boundary conditions are changed. One group of these modes (labeled "S" in Figs. 1 - 6) has predominantly shear wave characteristics, while the remaining thickness modes (labeled "D" in Figs. 1 - 6) form a group with predominantly dilatational wave character. This is particularly evident from the manner in which the frequency curves for each group are affected by the boundary conditions. Thus the S-mode curves for free and for supported boundaries are very nearly identical, while both of these are vastly different from the S curves for clamped boundaries (see the two sets of figures, 1 - 4 and 5 - 6). On the other hand, the D-mode curves for supported and for clamped boundaries are strikingly alike while both of these differ widely from the D curves for free boundaries[10] (see the two

---

[10] The similarity of the D curves of Fig. 1 to those of Figs. 3,6, despite the difference in boundary conditions, is due to the fact that in each of these cases the boundary conditions imply $n \dfrac{\lambda}{2} = b - a$, $n = 1, 2, 3. \ldots$, where λ is the (ill-defined) radial wavelength.

sets of figures, 3, 6 and 2, 4, 5).

These conclusions are fortified by an inspection of the machine calculations for each mode. For this discloses that indeed the S-modes have displacement and stress fields largely shear in character (terms involving B_1, B_2 dominate in Eqs. (1)-(4)) while the D-modes have displacement and stress largely dilatational in character (terms with A_1, A_2 dominate in Eqs. (1) - (4)).

It appears then that the eigenfrequencies of the S-modes and D-modes are astonishingly close to those of pure shear and pure dilatational waves, respectively (except for the lowest modes of very thick shells). To a lesser degree, the stress and displacement fields are similar to those of pure modes. Thus, it is clear that the shear and dilatational waves are only very weakly coupled by our boundary conditions, and that the "frequency mixing" is extremely small. These statements are, of course, exactly true for axially symmetric modes ($m = 0$ in Eqs. (1) - (4), also cf. ref. 4).

2. Gas-Filled Cylinder

We now turn to the mode maps for the three sets of boundary conditions given by Eqs. (9) with (10c), corresponding to a cylinder filled with a "stiff" gas, while its outer surface is either free, or supported, or clamped.

The numerical work was considerably more complicated here than for the cases described previously (Sec. V. 1). This is because the $\underline{f}$ vs $\underline{a}$ curves for the gas-filled cylinder are somewhat jagged, and at some points in the $\underline{f}$-$\underline{a}$ plane two modes come close together. The method of computation adopted was to trace out each mode curve separately as a function of $\underline{a}$, by a slope-projection technique. Where two modes approach each other closely, accidental jumping from one to the other was avoided by collapsing the interval until $Z'_g(k_g a)$ varied smoothly. We have done these calculations for several values of $\underline{m}$. In ref. 7, the mode maps for $m = 0$, clamped outer surface, and $m = 2$, clamped, supported or free outer surface, have already been presented. Here we display in Figs. 7 - 12 the mode maps for $m = 0, 1, 3$ not heretofore published.

The axially symmetric ($m = 0$), or pure radial modes are shown in Figs. 7, 8 for free and supported outer surface, respectively. We have plotted only the dilatational modes, since in this case, the shear modes are not coupled to the gas and thus are the same as in Figs. 1 - 6. As might be expected, the mode frequencies correspond rather closely to either the solid or gas quasi-modes, i.e., the modes of a solid shell with free inner surface, or the modes of a gas in a rigid walled cylinder, respectively. These quasi-modes, where
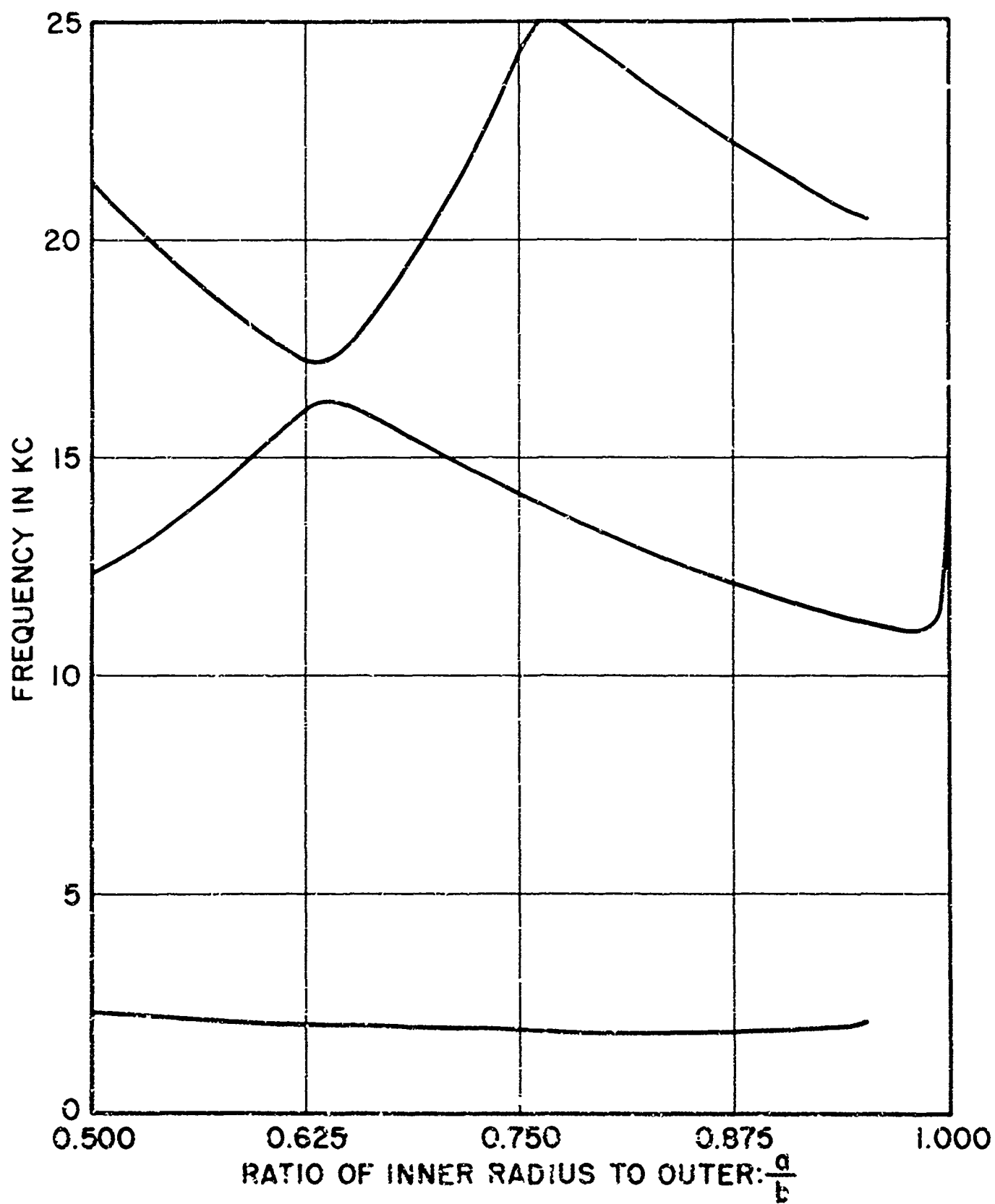
Fig. 7 FREQUENCY VERSUS GEOMETRY FOR THE RADIAL MODES (m=0)
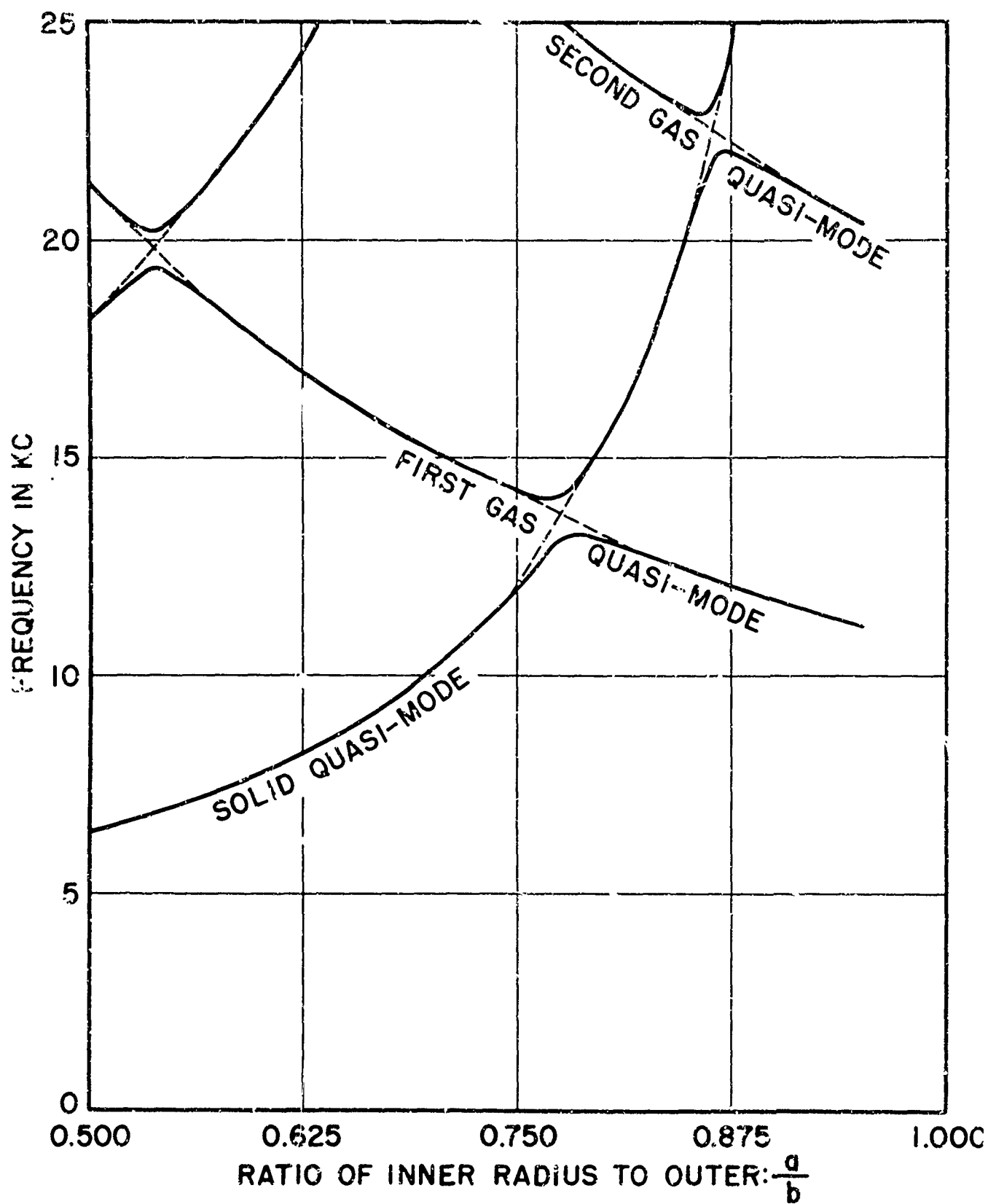OF THE GAS-FILLED CYLINDER WITH FREE OUTER RADIAL SURFACE

Fig. 8 FREQUENCY VERSUS GEOMETRY FOR THE RADIAL MODES
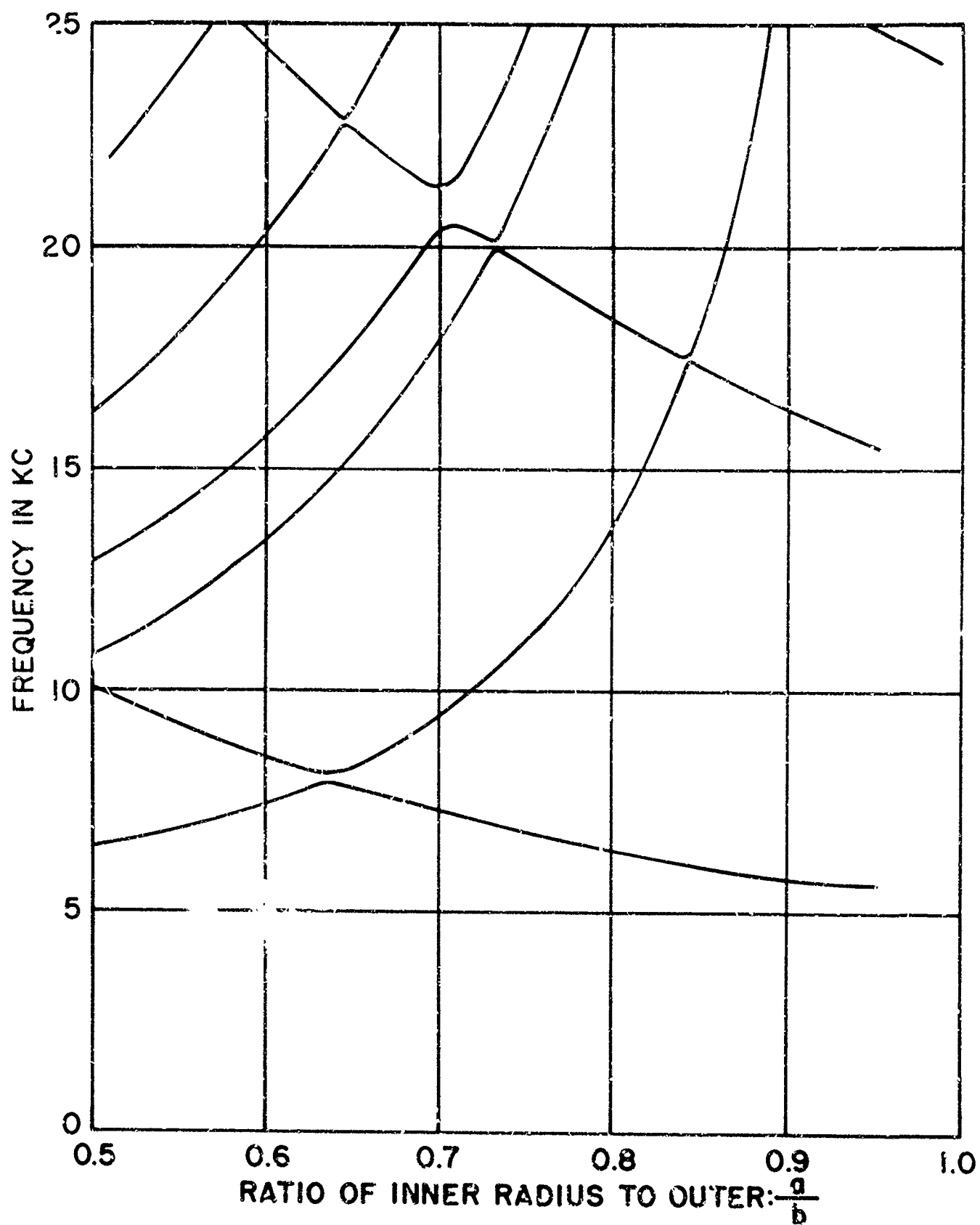(m ≈ 0) OF THE GAS-FILLED CYLINDER WITH SUPPORTED
OUTER RADIAL SURFACE

Fig. 9   FREQUENCY VERSUS GEOMETRY FOR THE FIRST AZIMUTHAL
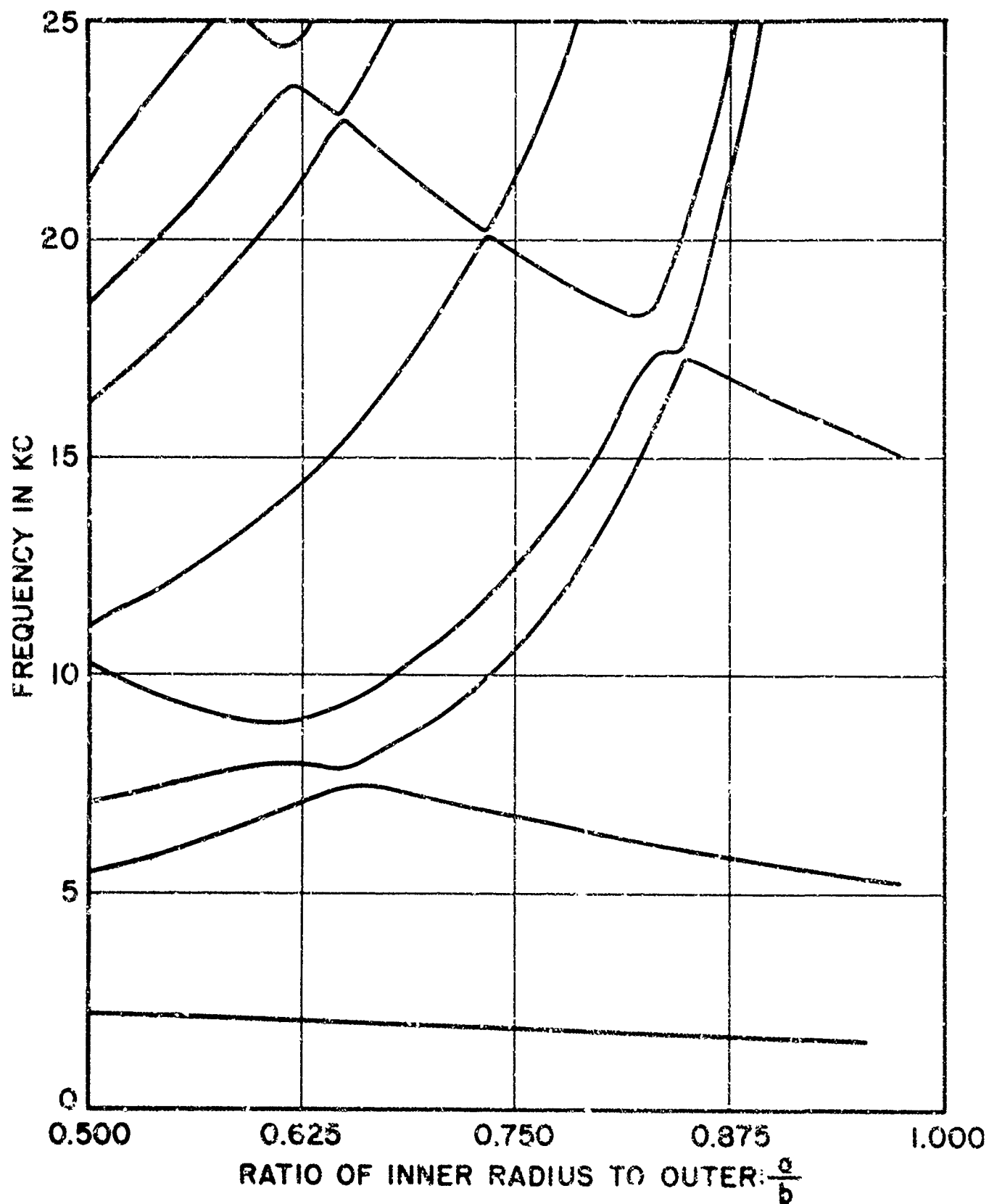MODES (m = 1) OF THE GAS-FILLED CYLINDER WITH FREE
OUTER RADIAL SURFACE

Fig. 10   FREQUENCY VERSUS GEOMETRY FOR THE FIRST AZIMUTHAL
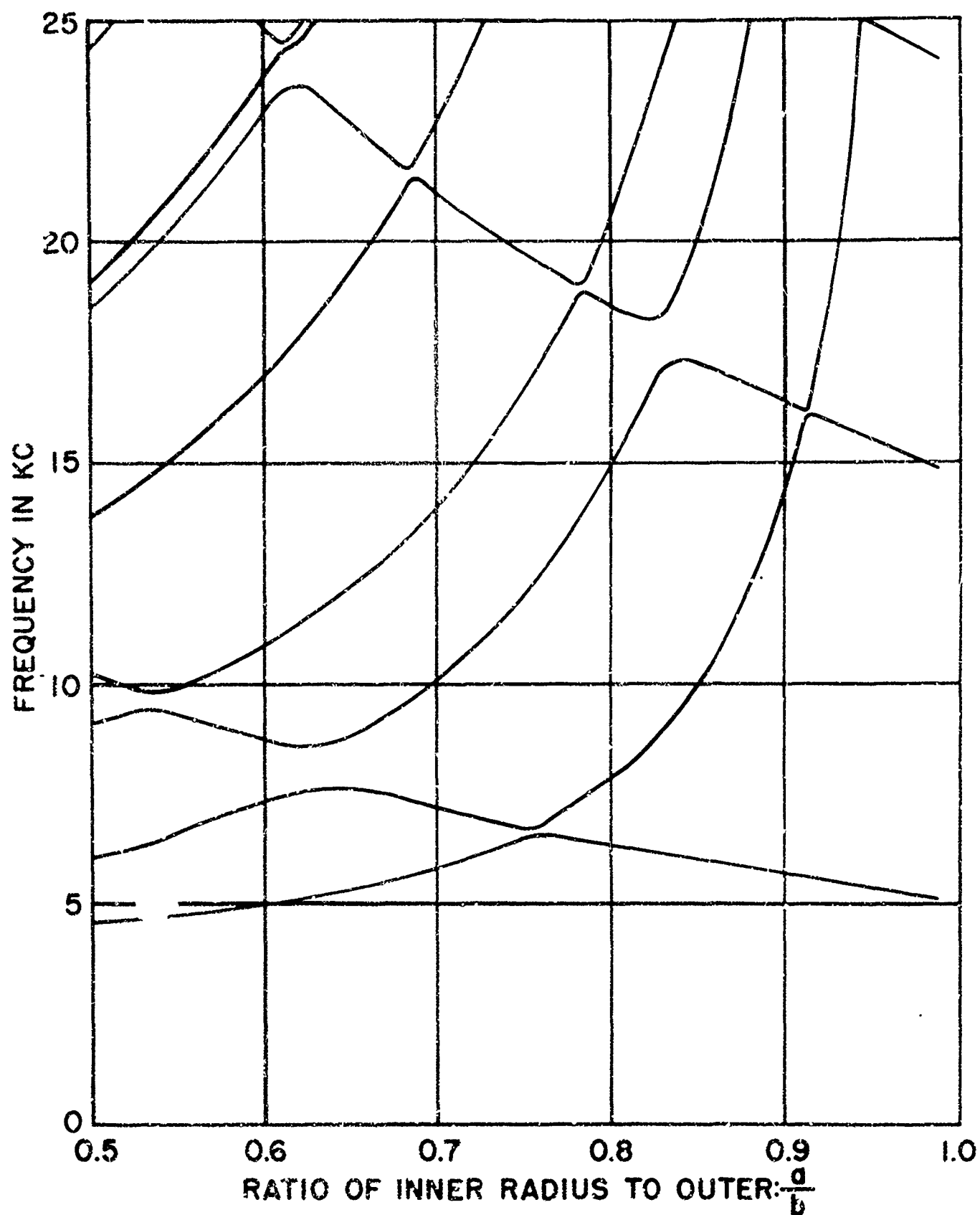MODES (m = 1) OF THE GAS-FILLED CYLINDER WITH SUPPORTED
OUTER RADIAL SURFACE

Fig. 11 FREQUENCY VERSUS GEOMETRY FOR THE FIRST AZIMUTHAL MODES (m = 1) OF THE GAS-FILLED CYLINDER WITH CLAMPED OUTER RADIAL SURFACE
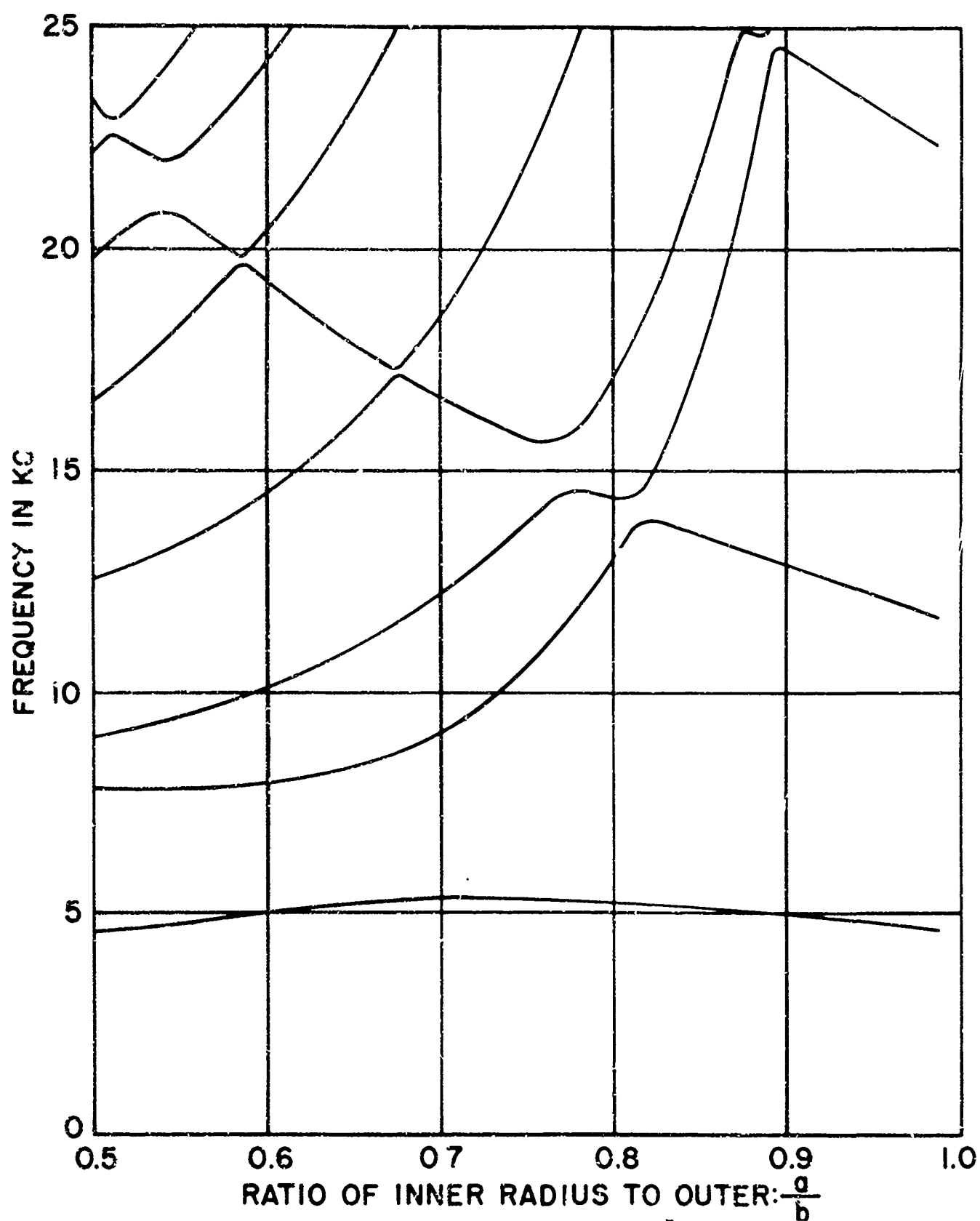
Fig. 12   FREQUENCY VERSUS GEOMETRY FOR THE m = 3 MODES OF THE
GAS-FILLED CYLINDER WITH SUPPORTED OUTER RADIAL SURFACE

different from the actual modes, are indicated, for example, by the dashed lines in Fig. 8. Since the interface boundary conditions for the quasi-modes are mutually exclusive, the modes of the two-phase system avoid the intersections of dashed lines, and alter their character in such neighborhoods from quasi-modes of one medium to those of the other.

Figs. 9, 10, 11 show the first azimuthal modes (m = 1) for free, supported and clamped outer surface, respectively. Here the modes of the two-phase system are not individually pure shear or pure dilatational, as they are when m = 0, but combinations of both, so that the mode-maps appear rather complicated. We note that the "splitting" of modes at gas quasi-mode and solid quasi-mode intersections is influenced not only by the mismatch in acoustic properties of the solid and the gas, but also by the relative amounts of shear and dilatational motion in the solid. For example, compare Fig. 11 with Fig. 5, where we see that where a gas quasi-mode intersects a type "D" solid quasi-mode, the splitting is much larger than where it intersects a type "S" solid quasi-mode. This may be presumed to occur because the gas exerts no shear on the solid, and couples directly only to the dilatational motion -- and, as we saw in Sec. V.1, the "S-modes" have little dilatational character, while the "D-modes" are largely dilatational. [11]

Finally, Fig. 12 shows the third azimuthal (m = 3) modes of the cylinder with supported outer radial surface.

---

[11] For further qualitative discussion of the modes of the two-phase system, see ref. 7b.

VI. ATTENUATION OF SOUND IN CYLINDER WALL

We shall now calculate the rate of dissipation of elastic wave energy in the wall of the gas-filled cylinder (cf. ref. 7a). In a stationary state, this is equal to the rate at which energy flows into the cylinder wall across the inner surface $(r = a)$,[12] so that, in the acoustic approximation, the dissipation rate per unit length of solid wall is

$$+ \frac{\pi a}{2} \, J_m^2 \, (k_g a) \, \left| p_0 \right|^2 \text{ Real part of } \left(\frac{i\omega S_r}{-P_{rr}} \right)_{r=a} ,$$

where p_0 is the gas pressure amplitude (Sec. III.2). The real part of the boundary admittance is given to first order in the coefficients of expansive friction (λ^1) and shear viscosity (η) by[7a]

$$\text{Re} \left(\frac{i\omega S_r}{-P_{rr}} \right)_a = - \omega^2 \left[\lambda^1 \frac{\partial}{\partial \lambda} + \eta \left(\frac{\partial}{\partial \mu} - \frac{2}{3} \frac{\partial}{\partial \lambda} \right) \right] \left[\frac{S_r}{-P_{rr}} \right]_a . \quad (12)$$

We note that, for the physical constants used in this work (Sec. IV), the first order expression (12) should be accurate to a few percent up to frequencies ~ 100 kc.

The derivatives in Eqs. (13) were calculated during the process of finding the characteristic frequencies of the gas-filled cylinder (Sec. V.2). Once the eigenfrequency for a given $\underline{a}$ was determined, λ (or μ) was varied slightly

---

[12]The energy flux at $r = b$ is zero for all boundary conditions treated in this paper (see Sec. III).

and, for the same $\underline{a}$ and the $\underline{\text{same frequency}}$, the coefficients A_1, A_2, B_1, B_2 were recalculated as minors of the secular determinant. The derivatives are then obtained from Eqs. (1), (3), and the real part of the boundary admittance from Eq. (12). The dilatational part of the damping ($\lambda^1 = 200$ poise, $\eta = 0$) and the total damping ($\lambda^1 = \eta = 200$ poise) are shown separately in the figures.

Some attenuation calculations for the $m = 2$ modes have already been presented in ref. 7a. Here we display the results for the $m = 0$ and $m = 1$ modes of the cylinder with supported outer surface (Figs. 13 and 14). The admittances are plotted as functions of a/b along those portions of the modes which are closest to the $\underline{\text{lowest}}$ gas quasi-mode (cf. Figs. 8 and 10), since they are very large except very close to the gas quasi-mode. In Fig. 15, we have plotted the admittance for a first azimuthal $\underline{\text{ring-mode}}$ (cf. lowest curve in Fig. 10) for the supported boundary at r = b. Note that the damping is about 10,000 times larger for the ring-mode than for the thickness modes.
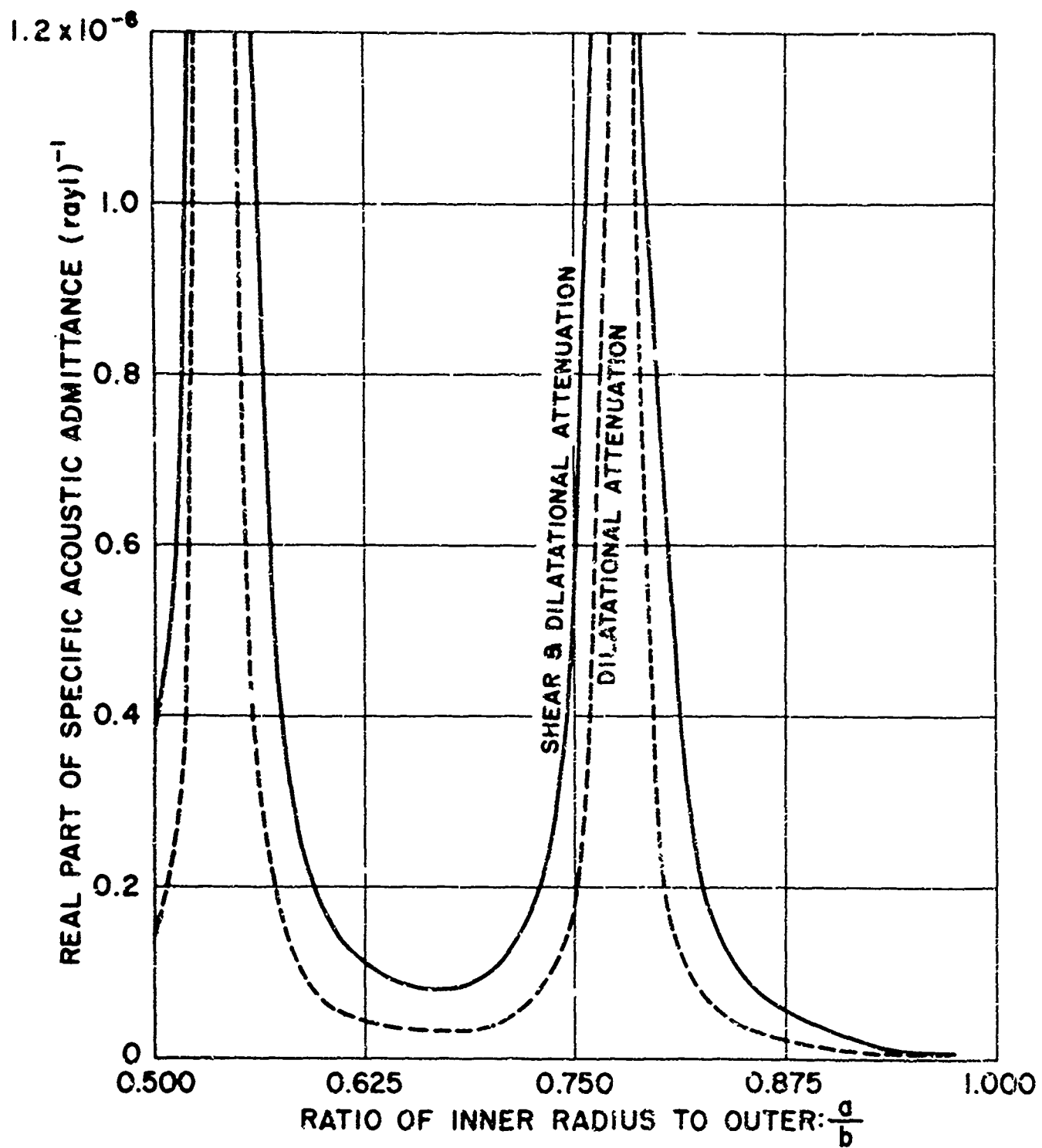
Fig. 13 ATTENUATION OF SOUND IN THE SOLID WALL OF THE GAS-
FILLED CYLINDER WITH SUPPORTED OUTER SURFACE
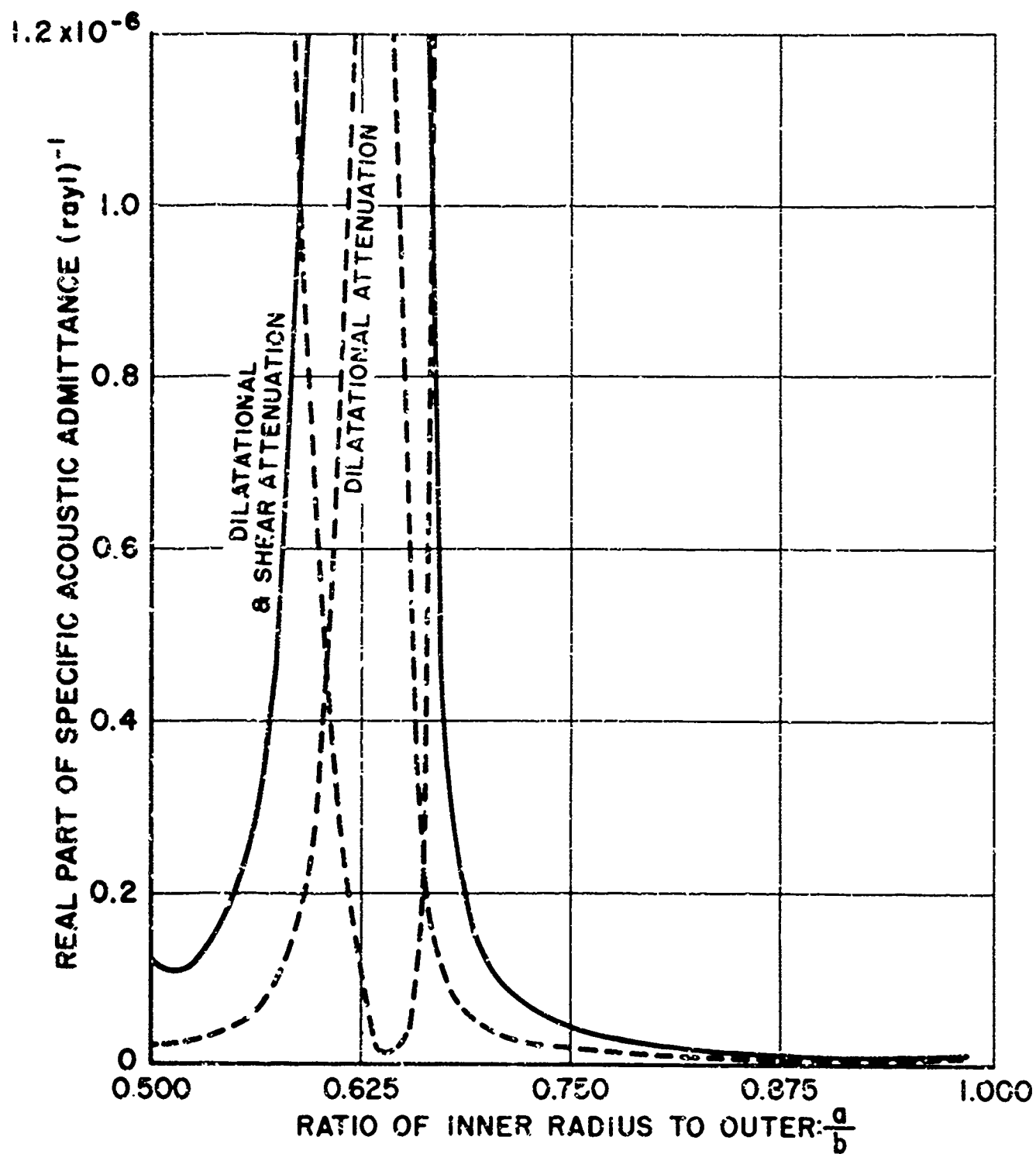FOR RADIAL MODES (m = 0) LYING NEAR TO THE
LOWEST GAS QUASI-MODE

Fig. 14 ATTENUATION OF SOUND IN THE SOLID WALL OF THE GAS-
FILLED CYLINDER WITH SUPPORTED OUTER SURFACE
FOR FIRST AZIMUTHAL MODES (m = 1) LYING
NEAR TO THE LOWEST GAS QUASI-MODE

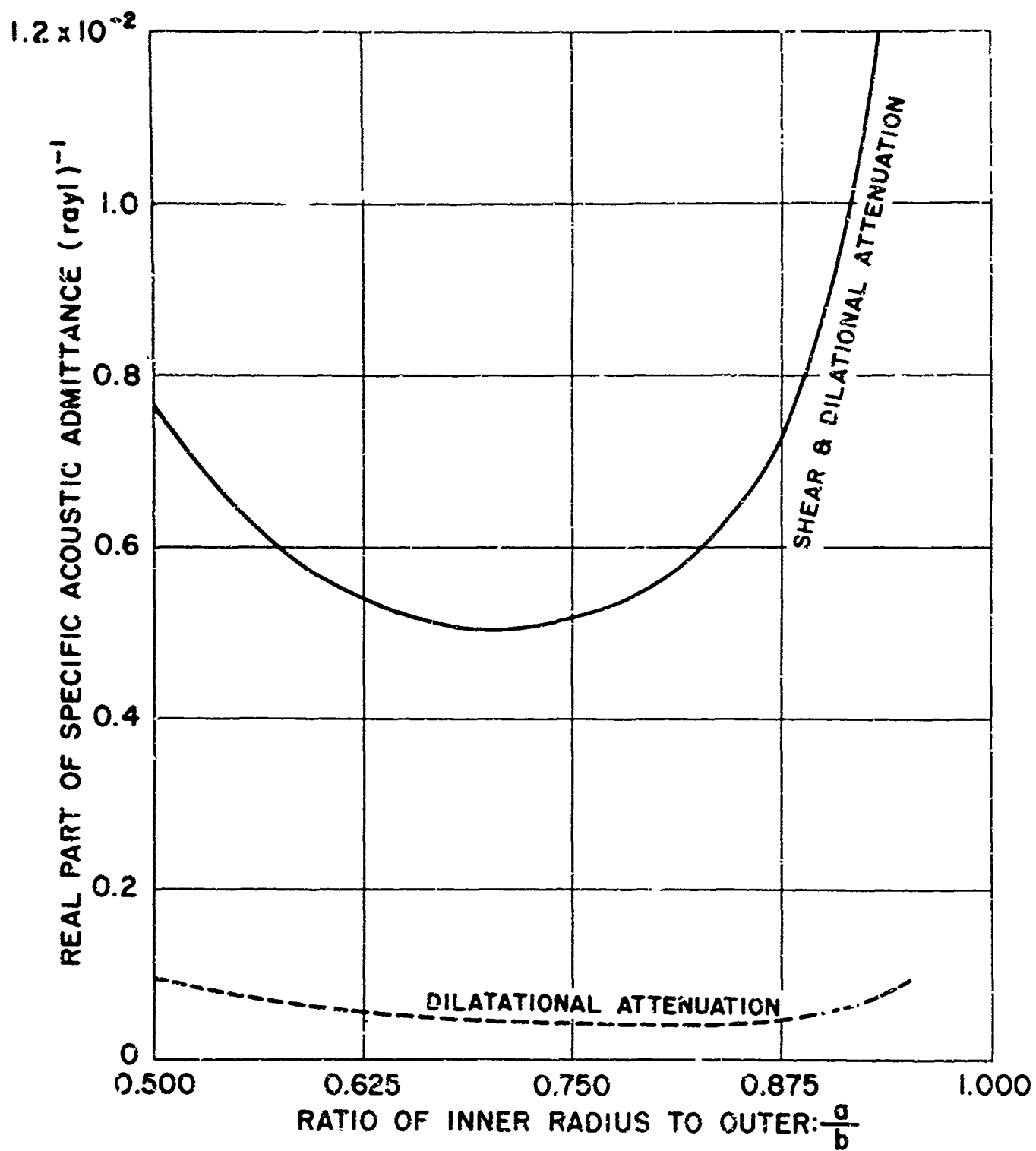Fig. 15   ATTENUATION OF SOUND IN THE SOLID WALL OF THE GAS-
FILLED CYLINDER WITH SUPPORTED OUTER SURFACE
FOR THE FIRST AZIMUTHAL (m = 1) RING-FLEXURAL
MODE

VII. CONCLUSION

In this paper we have been concerned primarily with exact calculation of the plane-strain eigenfrequencies of an infinitely long, hollow cylinder of arbitrary wall thickness. We have considered free, supported and clamped radial surfaces in heretofore unstudied combinations. In addition, we have presented new mode-maps (frequency vs geometry) for a gas-filled cylinder. Finally, we have evaluated the attenuation of sound energy in the thick cylindrical shell.

From a study of our results for the diverse boundary conditions it has appeared that the thickness eigenmodes may be regarded as consisting of two distinct classes, the first being almost purely radial dilatational waves, (D class), the second almost purely azimuthal shear waves, (S class). The sharpness of this dichotomy evidences very weak shear-compressional coupling, so that the thickness modes should be easily obtainable from the pure modes by perturbation theory. The development of such an approximate theory will be the topic of a subsequent paper by one of the authors.

The calculations for the gas-filled cylinder showed that the mode frequencies are very close either to those of the gas quasi-modes or to those of the solid quasi-modes, depending on the radial dimensions of the cylinder and the number of nodes in the radial direction.

ACKNOWLEDGMENT